The Journal of Experimental Biology 211, 766-772
Published by The Company of Biologists 2008
doi:10.1242/jeb.007658

# Elasticity, unexpected contractility and the identification of actin and myosin in lobster arteries

J. L. Wilkens[1,*], M. J. Cavey[1], I. Shovkivska[2], M. L. Zhang[2] and H. E. D. J. ter Keurs[2]

[1]Department of Biological Sciences, Faculty of Science, University of Calgary, 2500 University Drive N.W., Calgary, Alberta, T2N 1N4, Canada and [2]Department of Physiology and Biophysics, Faculty of Medicine, University of Calgary, 4440 Hospital Drive N.W., Calgary, Alberta, T2N 4N1, Canada

*Author for correspondence (e-mail: wilkens@ucalgary.ca)

Accepted 11 December 2007

## SUMMARY

**Lobster arteries, which exhibit non-uniform elasticity when stretched, have a trilaminar organization. The inner layer is an elastic connective tissue and the outer layer is a collagenous connective tissue; the middle layer of an artery is an aggregation of cells containing microfilaments. Arterial cells possess actin, myosin and tropomyosin. Except for the dorsal abdominal artery, striated muscle cells are not evident in the walls of any of the vessels. The neurotransmitter glutamic acid and the neurohormone proctolin elicit slow circumferential contractions in all of the arteries leaving the lobster heart. Only the dorsal abdominal artery contracts when stimulated electrically. Longitudinal strips of the arteries do not respond to either drugs or electrical stimulation. Arterial contraction will have profound effects on resistance to blood flow and may be an important component of the control mechanisms regulating blood distribution.**

Key words: actin, artery, cardiovascular system, lobster, microfilament, myosin, vascular resistance, *Homarus americanus*.

## INTRODUCTION

The circulatory system of decapod crustaceans consists of a single-chambered heart that pumps haemolymph (blood) into an array of seven arteries (McLaughlin, 1980). Muscular cardioarterial valves are present at the origins of six of the arteries (anterior median artery, AMA; anterior lateral arteries, ALAs; hepatic arteries, HAs; and sternal artery, SA), but not at the origin of the dorsal abdominal artery (DAA). At the back of the heart, a muscular flap is situated at the entry into the bulbus arteriosus (Kuramoto et al., 1992; McMahon et al., 1997). The DAA and the SA originate from the bulbus. Valves are also located at the origins of the segmentally paired lateral arteries that arise from the DAA (Davidson et al., 1998), but they have not been found at the branch points along any of the other vessels. Arteries divide until the finest arterioles terminate in capillary-sized tissue spaces (McGaw and Reiber, 2002) (J.L.W., unpublished observations on lobsters). Haemolymph collects in and returns to the heart through sinuses.

It seems imperative that a large crustacean be able to control the distribution of haemolymph to different regions of the body to accommodate changing physiological demands for oxygen, nutrients, and waste removal. Using pulsed-Doppler techniques on intact animals, such distributional control has indeed been observed in response to hypoxia (Airriess and McMahon, 1992) and after feeding (McGaw and Reiber, 2000; McGaw, 2005).

There are several possible mechanisms for controlling flow patterns among the arteries. The cardioarterial valves are innervated (Fujiwara-Tsukamoto et al., 1992), and they are responsive to a variety of cardioactive drugs (Kuramoto et al., 1995; Wilkens and Kuramoto, 1998). In addition, the arteries, if perfused with cardioactive drugs at a point distal to the cardioarterial valve, show increased resistance to flow (Wilkens, 1997; Wilkens and Taylor, 2003). For the DAA, the sites of drug action could be the striated muscle blocks in its lateral walls (Martin et al., 1989; Wilkens et al., 1997b) as well as the valves at the branch points to the lateral arteries (Davidson et al., 1998). The other arteries do not have either striated muscle in their walls (Wilkens et al., 1997b; Chan et al., 2006) or valves along their length. To date, all other contractile (skeletal, cardiac and intestinal) tissues in crustaceans have been shown to be striated muscles. It has been assumed that crustacean arteries, with the possible exception of the DAA, are passive capacitance vessels. The goal of the present study was to determine if lobster arteries are purely passive vessels or whether they possess active properties.

## MATERIALS AND METHODS

### Animals and dissection

Clawed lobsters, *Homarus americanus* H. Milne Edwards 1837, were purchased from a local wholesaler and maintained in a sea water aquarium at 14°C. Prior to dissection, animals were 'cold' anesthetized by burial in crushed ice for about 30 min. They were then pithed by crushing the supra-oesophageal ganglion. The carapace over the heart was removed, and the heart was perfused with chilled saline to clear the arteries of haemolymph. Chilling and cold saline slowed the clotting reaction. After a 10–15 min wash, the dissection continued to expose the arteries. The arteries used were the ALAs, the HAs, the SA and the DAA. The circumference of the AMA was measured, but the vessel was too small to be used in our apparatus. Ostial muscle (OOM; orbicularis ostii) was used to compare arteries to a known cardiac muscle (Yazawa et al., 1999). Arteries and OOM were stored in ice-chilled saline and tested over 2 days. The lobster saline used for dissection and perfusion contained (in mmol $l^{-1}$) 479.6 NaCl, 15.7 KCl, 25.9 $CaCl_2$, 9.3 $MgSO_4$ and 5.0 Tris buffer; the saline was equilibrated with air and adjusted to pH 7.6.

## Morphology and morphometry

### Histochemistry

SAs were excised, cut longitudinally with iridectomy scissors, and opened onto cover glasses. The spreads were ringed with petroleum jelly and flushed with saline. A solution of 3.7% formaldehyde in saline was added to the reservoirs for 10 min. The spreads were then washed with saline (2 min), permeabilized with 0.1% Triton X-100 (5 min), washed with saline (2 min), incubated in 1% bovine serum albumin in saline (30 min), stained with a double-strength stock of Rhodamine–phalloidin (catalogue no. R-415; Molecular Probes, Eugene, OR, USA) for 30 min, and washed with saline (2 min). Rhodamine–phalloidin is a fluorescent phallotoxin probe for fibrous (F) actin (Wieland, 1986). The cover glasses were inverted and mounted on microscope slides with a solution of equal parts of glycerol and saline. As a control, the Rhodamine–phalloidin was omitted from the protocol.

SA spreads were viewed and photographed with a Nikon Eclipse TE300 inverted fluorescence microscope. The microscope was calibrated with a stage micrometer (100 lines $mm^{-1}$), and photomicrographs were made with Kodak Ektachrome 100 film. The transparencies were digitized with a Polaroid SprintScan 45i film scanner at a resolution of 600 dpi, and the images were stored as uncompressed TIFF files. Image files were converted to grayscale, adjusted, and printed with 'Photoshop CS2 for Windows' (9.0) software (Adobe Systems, San Jose, CA, USA).

### Ultrastructure

SAs destined for histology and ultrastructure were processed at slack length. The isolated vessels were cannulated and perfused and bathed with phosphate-buffered glutaraldehyde (Cloney and Florey, 1968) for 5 min. The arteries were cut into short cylindrical segments, and these rings were transferred to a container of fresh fixative, where they remained for 60 min at room temperature.

The aldehyde-containing fixative was decanted, and bicarbonate-buffered osmium tetroxide (Wood and Luft, 1965) was added to the container. The container was placed in an ice bath for 60 min. At the end of osmication, the arterial rings were rinsed with demineralized water, dehydrated with graded solutions of ethanol, and treated with propylene oxide. The rings were infiltrated and embedded in LX-112 epoxy resin (Ladd Research Industries, Williston, VT, USA).

Ultrathin sections (70–80 nm in thickness), cut with a diamond knife on a Sorvall MT-6000 ultramicrotome, were collected on unsupported copper grids and stained with aqueous solutions of uranyl acetate (saturated) and lead citrate (Reynolds, 1963). The sections were viewed with an Hitachi H-7000 transmission electron microscope operated at 75 kV and equipped with an SIA-8A digital camera (Scientific Instruments and Applications, Duluth, GA, USA). The microscope was calibrated with a carbon replica of a diffraction grating (2158 lines $mm^{-1}$), and digital images were captured at a resolution of 2048×2048 pixels and saved as uncompressed TIFF files. Image files were adjusted and printed with 'Photoshop CS2 for Windows' (9.0) software.

### Morphometry

Some aldehyde-fixed arterial rings were transferred to saline for examination with a Nikon SMZ800 stereomicroscope. The microscope was calibrated with a stage micrometer. The rings, ranging in length from 0.5 to 1 mm, were oriented on end and photographed with a Nikon Coolpix 5000 digital camera using both reflected and transmitted light. The images were captured at a resolution of 2560×1920 pixels and saved as uncompressed TIFF files. Image files were imported into 'SigmaScan Pro for Windows' (5.0) software (Systat Software, Point Richmond, CA, USA) for morphometric analysis of wall thickness and luminal area. Ten measurements of wall thickness and two measurements of luminal area were made on each ring. Luminal (inside) diameter was calculated by treating the luminal area as the area of a circle. Alternatively, rings were cut open longitudinally and spread onto microscope slides; cover glasses were mounted with saline. The slack circumference of a vessel was measured as the width of the specimen, measured with an ocular micrometer (10 lines $mm^{-1}$) in a Wild Heerbrugg M5 stereomicroscope.

## Biochemistry

Arterial rings (6 mm long), OOM, slow skeletal muscles from the crusher claw and fast skeletal muscles from the cutter claw were homogenized in 40 μl sodium dodecyl sulfate (SDS) sample buffer. The sample buffer was kept in an ice bath. Protein electrophoresis of the homogenates was carried out on 12% SDS-polyacrylamide discontinuous Laemmli gels (16×20 cm) for use in a Bio-Rad Mini-Protean electrophoresis system (SDS-PAGE).

## Physiology

Arterial wall and OOM force was measured using a strain gauge (resonant frequency 286 Hz, SensoNor AE801; Sensor One, Sausalito, CA) connected to a Gould Bridge amplifier. Rings, 1–2 mm in length, and longitudinal strips were cut from the arteries. Insect pins glued to the force transducer and an ergometer were placed inside a ring or inserted into the ends of a strip. The manipulator-mounted transducer was moved to apply a small stretch to the arterial wall. The linear compliance component of the transducer wafer and insect pin (0.167 mm $mN^{-1}$) was measured from the force while the manipulator moved the pin against a rigid stop. After a stretched ring had relaxed to equilibrium (relaxation time constant, $\tau$=1/e, 7–16 s, depending on the magnitude of the stretch), the active force generated in response to drugs or electrical stimulation was determined. Tissues were stimulated electrically with a pair of laterally placed platinum ribbon electrodes. Arteries were stimulated with repeated 2 ms pulses delivered at 20 Hz. OOM received trains of stimuli (2 ms pulses delivered at 20 Hz, 100 ms train duration, 2 trains $min^{-1}$). Data were recorded using a PowerLab/4SP A-D converter (sampling rate 100 Hz to 2 kHz) and analyzed with 'Chart for Windows' (4.2) software (ADInstruments, Colorado Springs, CO).

The passive force–length and stress–strain relationships were determined for three arteries to evaluate their relative compliance and to determine the magnitude of diameter change that a contraction would produce. Strain was defined as stretch ($\Delta l$) divided by slack circumferential length ($L_o$), and stress was defined as force divided by wall area (ring length multiplied by wall thickness).

The preparation was continuously superfused with saline at 12°C (4 ml $min^{-1}$ in a 1.5 ml bath). The source to the superfusion pump could be switched between normal saline and saline containing the neurotransmitter glutamic acid (GLU, 10 mmol $l^{-1}$; Sigma Chemical Co., St Louis, MO) or the neuropeptide hormone proctolin (PR, 1.0 μmol $l^{-1}$; Sigma Chemical Co.). These concentrations were effective in causing increased flow resistance in perfused arteries (Wilkens, 1997; Wilkens and Taylor, 2003) and contraction in OOM (Wilkens et al., 2005). Although the GLU level appears high, it may reflect the effective concentration in glutaminergic synapses. Drug exposure was continuous until a response reached a stable maximum, often requiring more than 5 min.

The actin inhibitor cytochalasin D (CD; Sigma Chemical Co.) was tested on arterial rings and OOM pretreated for 5–10 min at concentrations from 0.5 to 10.0 μg ml$^{-1}$. Since rings recovered extremely slowly (>90 min) from drug-induced contractions, successive rings were used for each test (e.g. rings one and three would be exposed to PR and ring two would be pretreated with CD and then exposed to PR diluted in the same concentration of CD).

Statistical comparisons between data sets were performed using Student's *t*-test. Differences where $P<0.05$ were considered significant.

## RESULTS

### Morphology

The arteries leaving the heart of the lobster are trilaminar vessels consisting of a tunica interna, a tunica intermedia and a tunica externa (Chan et al., 2006). The tunica interna is an elastic connective tissue adjoining the lumen of the vessel, and the tunica externa is a collagenous connective tissue anchoring the vessel to the adventitia of the body. The highest concentration of cells is found in the tunica intermedia. In the small vessels (ALAs, AMA and HAs) leaving the anterior end of the heart, the cells of the tunica intermedia aggregate into compact masses. In the larger vessels (SA and DAA) departing from the rear of the heart, the cells of the tunica intermedia are less compacted, being infiltrated by connective-tissue elements and, in the case of the DAA, by blocks of striated muscle cells.

Cells in the tunica intermedia of the ALA (Chan et al., 2006), the AMA (Cavey et al., 2008) and the SA (present study) stain intensely after exposure to Rhodamine–phalloidin (Fig. 1A), correlating with the presence of bundled microfilaments in the cells of this layer (Fig. 1B). These microfilament bundles traverse the cytoplasm and frequently associate with filamentous mats on the inner surface of the plasmalemma.

### Biochemistry

Although microfilament bundles are apparent in transmission electron micrographs, and the actin content of these filaments is confirmed by Rhodamine–phalloidin staining, there is no morphological evidence of myosin. SDS-PAGE showed clear protein bands at the molecular masses for myosin (230 kDa) and actin (43 kDa) in the striated muscle-containing DAA and OOM, the slow and fast skeletal muscles, and the ALA and SA (Fig. 2). These bands corresponded in position to those identified by Medler and Mykles (Medler and Mykles, 2003) when position of the molecular marker distribution had been scaled for P75 and actin. The band labelled P1, 2 at ~105 kDa may represent paramyosin. The myofibrillar protein P75 was present in fast, but not slow, skeletal muscle. Numerous other bands are common to the different homogenates, but we did not attempt to identify them.

### Physiology

Several characteristics of the lobster cardiovascular system are provided for reference: animal mass 618±41 g, $N=8$; resting heart rate 61±4 beats min$^{-1}$, $N=8$; systolic pressure 2.532 kPa, $N=2$; diastolic pressure 0.533 kPa, $N=2$; pericardial sinus pressure 1.002 kPa, $N=2$; dorsal coelomic pressure 0.848 kPa, $N=2$; and arterial transmural pressure 1.654 kPa, $N=2$. Other physical properties of the arteries are provided in Table 1. Fig. 3 shows the circumferential stress–strain plots for the three arteries. The ALA, having the thinnest wall, is the least extensible, whereas the DAA is the most extensible.

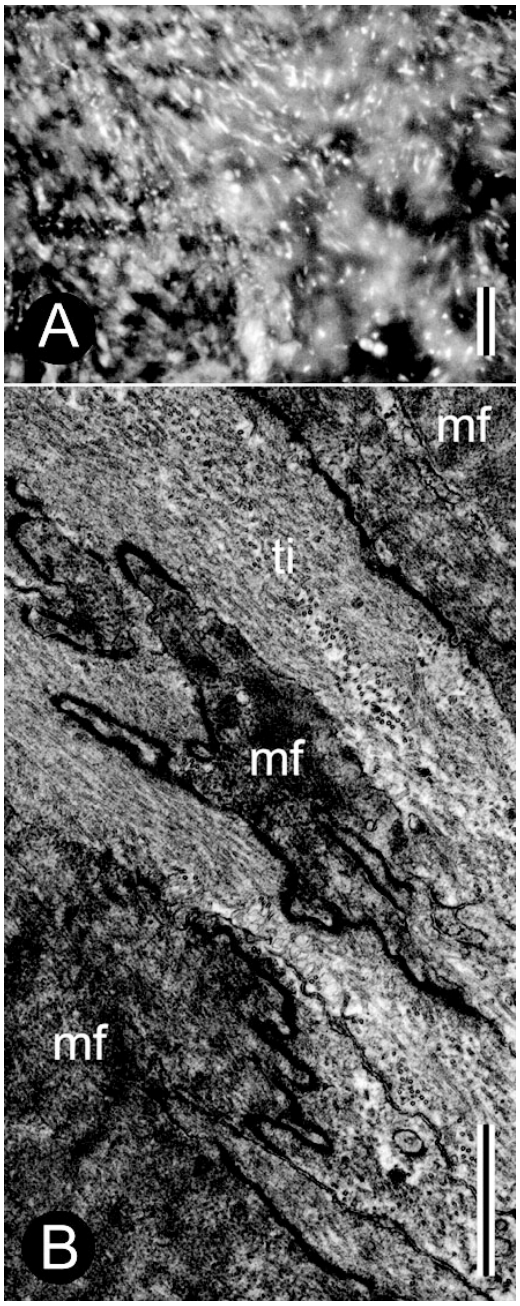


Fig. 1. Sternal artery. (A) Arterial spread treated with Rhodamine–phalloidin. Staining of the cells in the middle layer (tunica intermedia) of the vessel is strong. Scale bar, 100 μm. (B) Horizontal electron micrograph of an artery where the inner layer (ti, tunica interna) interfaces with the tunica intermedia. Bundles of microfilaments (mf) appear in the cortical cytoplasm and account for the fluorescence of cells in the tunica intermedia. Individual microfilaments are ~6.5 nm in diameter. Dense filamentous mats are applied to the inner and outer surfaces of the plasmalemmata. Scale bar, 1 μm.

Arterial rings slowly contracted upon perfusion with PR or GLU (Figs 4, 5; Table 2). These contractions often required 5–8 min to reach a maximum; recovery was much slower and proportional to drug exposure time, requiring more than 90 min after a 5 min drug treatment. The magnitude of the contractions varied from 0 to as much as 50% of the original passive equilibrium force. In the DAA, drug-induced changes in force could have arisen from either the

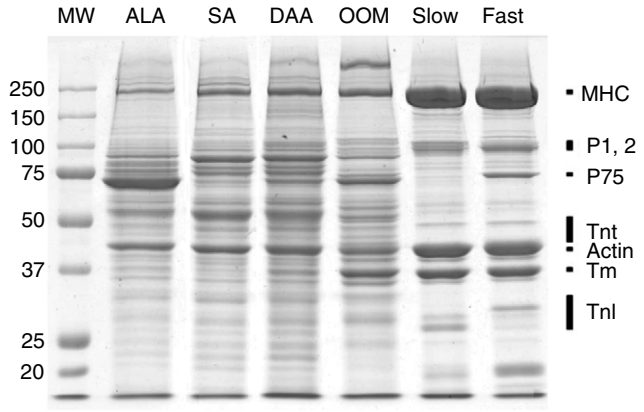


Fig. 2. SDS-PAGE of three arteries (ALA, SA and DAA), the ostial muscle (OOM), and the slow and fast skeletal muscles, shows bands identified as actin, myosin and tropomyosin. The left-hand lane (MW) contains protein markers of known molecular mass (in kDa). Labelled on the right are myosin heavy chain (MHC), paramyosin (P1, 2), P75 in fast skeletal muscle, actin, tropomyosin (Tm), and troponins T (TnT) and I (TnI).

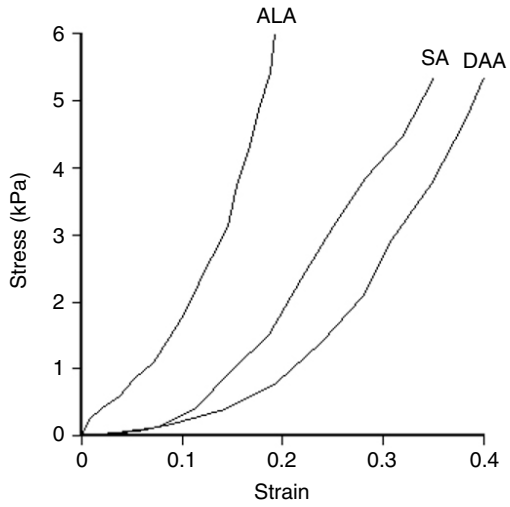


Fig. 3. Stress–strain plots of three arteries. Strain was obtained by dividing the increments of stretch, $\Delta l$, by the unstretched circumference, $L_o$. For stress (kPa), the passive force (in mN) is divided by the cross-sectional wall area (longitudinal ring width multiplied by wall thickness).

striated muscle cells or the muscle-free areas of the vessel wall. The amplitude of PR-induced contractions was similar to that during electrical stimulation, but the rate of rise of force was much lower, requiring 20 s to reach peak active force during electrical stimulation and more than 5 min during PR exposure (Fig. 5; Table 2). The rate and amplitude of GLU-induced contractions of a DAA ring were greater than for PR and could represent responses of both the muscle and the muscle-free regions. None of the other arteries contracted when stimulated electrically. Longitudinal strips of arteries did not exhibit force generation during exposure to PR or GLU or during tetanic electrical stimulation. Similar tests were performed on OOM; GLU (data not shown), PR, and electrical stimulation caused large contractions that reached maximum values in seconds, as opposed to minutes for the arterial rings (see Fig. 7A,C).

Will the contractile force generated by an arterial ring be sufficient to alter vessel radius and, thus, the resistance to haemolymph flow? One estimate was taken from force-length relationships of rings. After the rings were incrementally stretched, the stretch was reduced to 2–2.3×$L_o$ where the passive force was in the range of transmural force and drugs were applied (Fig. 6). As shown for the SA in the middle panel of Fig. 6, the magnitude of contractile force was used to evaluate how much this force would

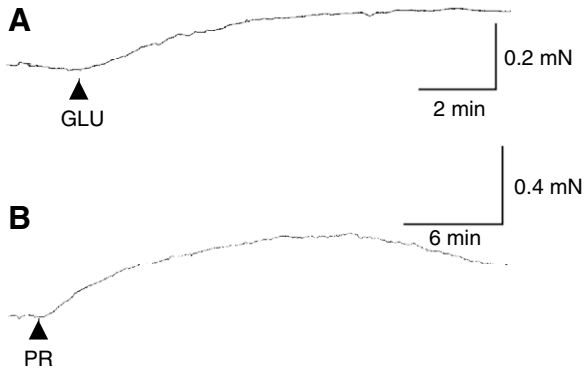


Fig. 4. (A) Response of a hepatic artery (HA) ring to continuous superfusion with glutamic acid (GLU; 10 mmol $l^{-1}$). Wall force at the time of GLU application was 0.170 mN. (B) Response of a sternal artery (SA) ring, at an initial wall force of 0.914 mN, to continuous superfusion with proctolin (PR; 1.0 μmol $l^{-1}$).

Table 1. Physical measurements of the cardiovascular system and responses to cardioactive compounds

| Artery | Outside diameter (mm) | *N* | Wall thickness (mm) | *N* | Radius change to PR or GLU (%) | *N* |
|---|---|---|---|---|---|---|
| AMA | 0.74±0.27 | 4 | | | | |
| ALA | 1.27±0.26<br>1.24* | 5 | 0.098±0.007<br>0.30* | 4 | PR: 13.6±6.0 | 3 |
| HA | 1.12±0.24 | 5 | | | | |
| SA | 1.91±0.30<br>3.60* | 4 | 0.229±0.006<br>0.09* | 4 | PR: 36.8±27.0 | 3 |
| DAA | 0.82±0.32<br>1.90* | 5 | 0.246±0.009<br>0.08* | 4 | PR: 36.8±27.0<br>GLU: 24.8±19.2 | 3<br>3 |

ALA, anterior lateral artery; AMA, anterior median artery; HA, hepatic artery; SA, sternal artery; DAA, dorsal abdominal artery.
*ALA and SA from the crab *Cancer magister* and DAA from the lobster *Homarus americanus* (Shadwick et al., 1990).

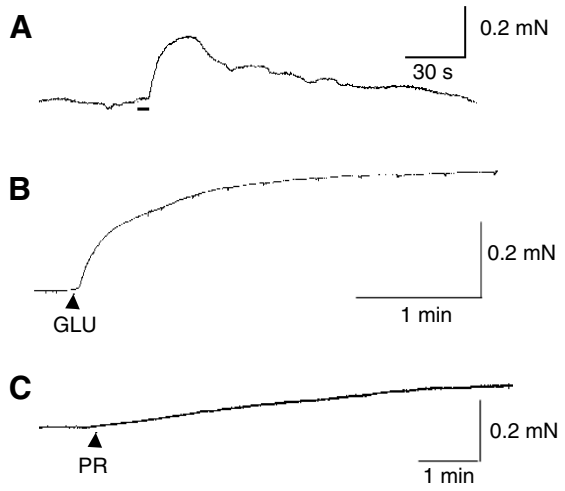


Fig. 5. Contraction of a dorsal abdominal artery (DAA) ring in response to (A) electrical stimulation (bar, 5 ms pulses, 20 Hz, 5 s duration) and (B,C) continuous superfusion with (B) glutamic acid (GLU; 10 mmol $l^{-1}$) and (C) proctolin (PR; 1.0 μmol $l^{-1}$).

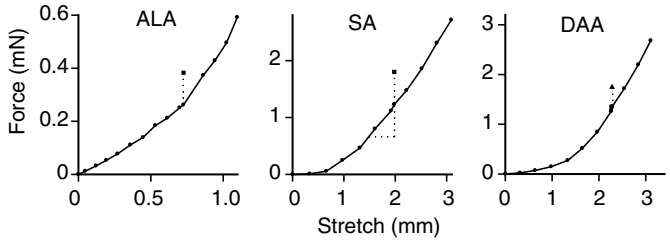


Fig. 6. Force–extension relationships for anterior lateral artery (ALA), sternal artery (SA) and dorsal abdominal artery (DAA) rings. The response to gradual stretch was determined first. Then, the length was reduced from maximum stretch to the test length where PR (proctolin; squares) or glutamic acid (GLU; triangles) was applied. The DAA response to PR is almost buried in the curve. The amount that the drug-induced contraction would have shortened the ring if it were free to move was determined as shown for the SA.

have decreased the circumference of the ring. From the responses of three animals so tested, PR would have reduced ALA, SA and DAA radii by 13.6±6.0, 36.8±27.0 and 6.3±3.8% (mean ± s.e.m.), respectively, and GLU would have caused a 24.8±19.2% reduction in DAA radius. These values are similar to or greater than those shown in Table 2, where drugs were tested over greater length ranges. Alternatively, contractile force will shorten a ring due to the transducer compliance. The PR-induced shortening of arteries shown in Fig. 6 would have reduced the radius for the ALA, SA and DAA by 5.1%, 5.2% and 2.7%, respectively. GLU reduced the radius of the DAA by 4.1%. This calculated amount of circumferential shortening may underestimate the shortening *in vivo*, because shortening in these experiments occurred against the compliant transducer.

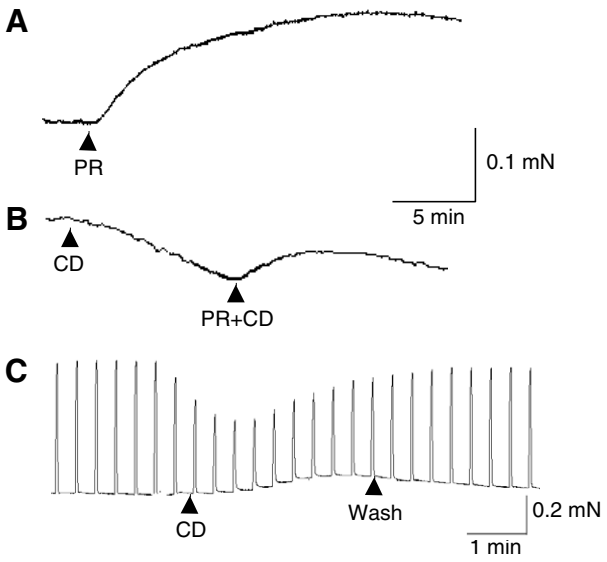


Fig. 7. Effect of cytochalasin D (CD; 0.5 μg $ml^{-1}$) pretreatment on a sternal artery (SA) ring and an ostial muscle (OOM). (A) Contraction of an SA ring in response to continuous perfusion with proctolin (PR; 1.0 μmol $l^{-1}$). (B) Effect of CD pretreatment on a PR-induced contraction in an adjacent SA ring. (C) Effect of CD (2.5 min) on basal tonus and electrically stimulated tetanic contractions of an OOM.

We explored the effect of cytochalasin D in order to study the involvement of microfilaments in generation and maintenance of the PR-induced force by these arteries. Pretreating with CD prevented PR-induced contraction in two ALAs, whereas five untreated rings contracted. For the SA, CD abolished or reduced PR-induced contraction in three of six rings taken from two animals (Fig. 7A,B). One of the SAs that failed to respond to PR during CD treatment contracted – but only weakly – when perfused with PR following 80 min of washing. CD (0.5 or 1.0 μg $ml^{-1}$, 5–10 min) treatment caused an irreversible decrease in tonus and a decrease in tetanic force in each of five OOMs from two animals. CD effects on OOM were reversible when exposure was of shorter duration (Fig. 7C).

Table 2. Effects of proctolin, glutamic acid and tetanic electrical stimulation on force development by arterial rings and orbicularis ostii muscle

| Tissue | Initial* | PR | *N* | Initial* | GLU | *N* | Initial* | Electrical stimulation | *N* |
|---|---|---|---|---|---|---|---|---|---|
| ALA | 0.502±0.047 | 0.055±0.010 (10.9%) | 12 | 0.693±0.168 | 0.011±0.004 (1.5%) | 2 | | 0 | 3 |
| HA | 0.201±0.070 | 0.010±0.015 (5.1%) | 5 | 0.173 | 0.165 | 1 | | 0 | 3 |
| SA | 0.681±0.332 | 0.136±0.163 (19.9%) | 12 | 0.613±0.106 | 0.060±0.038 (9.7%) | 5 | | 0 | 5 |
| DAA | 1.588±1.247 | 0.888±0.094 (5.7%) | 6 | 1.351±0.892 | 0.205±0.225 (15.2%) | 8 | 2.073±0.493 | 0.040±0.007 (1.9%) | 7 |
| OOM | 0.585±0.196 | 0.388±0.200 (66.3%) | 5 | 0.679 | 0.112 (16.4%) | 1 | 0.226±0.127 | 0.980±0.418 (433.6%) | 3 |

ALA, anterior lateral artery; HA, hepatic artery; SA, sternal artery; DAA, dorsal abdominal artery; OOM, orbicularis ostii muscle; PR, proctolin; GLU, glutamic acid.

*The force (in mN) at the time of drug administration or electrical stimulation. Values in the adjacent columns to the right are the incremental responses to a particular stimulus; percentage change from initial value shown in parantheses. All force values (mean ± s.e.m.) are expressed in mN.

## DISCUSSION

To date, skeletal, cardiac, and intestinal muscles of crustaceans (Factor, 1995; To et al., 2004), including those in the lateral walls of the dorsal abdominal artery (DAA) (Martin et al., 1989; Wilkens et al., 1997b), have proved to consist of striated cells. It has been assumed that other crustacean arteries only serve as haemolymph conduction vessels since electron micrographs reveal no evidence of muscle cells (Chan et al., 2006; Wilkens et al., 1997b). However, we know that several cardioactive compounds do increase the resistance to flow in *in situ* perfused arteries (Wilkens, 1997; Wilkens and Taylor, 2003). Although seemingly unlikely, it was important to determine whether these cardioactive agents could cause arteries to contract.

Rings of the anterior lateral artery (ALA), sternal artery (SA) and DAA exhibit non-linear elasticity, characteristic of the interplay of elastic and collagenous connective tissues, as are found in the tunica interna and the tunica externa, respectively (Shadwick et al., 1990; Wilkens et al., 1997a; Chan et al., 2006) (present study). Although vessel diameters are similar, the wall thicknesses reported here are 2–3.7 times greater than those cited previously for the crab and the lobster (Shadwick et al., 1990).

ALAs, HAs and SA do develop force when stimulated by proctolin (PR) and glutamic acid (GLU), observations suggesting that the cells with actin-based microfilaments also contained myosin. Protein analysis by SDS-PAGE demonstrated that actin and myosin are present in all three arteries as well as the cardiac ostia (OOM), and the slow and fast skeletal muscle. In addition, there are bands in all of our homogenates that correspond to paramyosin (P1, 2, ~105 kDa), tropomyosin (38 kDa), and troponins T and I (Fig. 2). The bands correspond closely with those found in skeletal muscle by Medler and Mykles (Medler and Mykles, 2003). For slow and fast skeletal muscles in lobsters, there are differences in the isoforms of myosin heavy chains (S1, S2, and fast) and tropomyosin (S1, S2, and fast) and the protein P75 which is found in fast but not in slow skeletal muscle (Meiss et al., 1981; Mykles, 1985; Medler and Mykles, 2003); however, these isoform differences are not distinguishable in our gels.

A clear distinction must be made between the DAA, with striated muscle cells in its architecture (Wilkens et al., 1997b), and the other six arteries. Consistent with the presence of muscle, DAA rings (but not longitudinal strips) contract during electrical stimulation; none of the other arteries respond to electrical stimulation. The striated muscle cells of the OOM contract rapidly when stimulated electrically.

Rings of all arteries contract during exposure to cardioactive drugs. Since the responses are clear and reproducible, they represent a reactive property of the vessels. PR induces stronger contractions in both ALA and SA than does GLU, whereas the reverse is true for the DAA, presumably reflecting different mechanisms of action of the different drugs on the muscle. Contraction probably arises from the formation of cross-bridges and will affect the resistance to flow in these arteries. The time course of the contractions is slow but similar to the changes in resistance to flow (approx. two- to threefold) seen in perfused arteries *in situ* (Wilkens, 1997; Wilkens and Taylor, 2003).

It is noteworthy that arteries taken from at least half of the animals were more responsive to PR and GLU 1 or 2 days after removal from the animal than on the day of dissection. The vessels *in vivo* may exist in a tonically 'contracted' state, a state that relaxes slowly once the tissues have been removed from the *milieu interieur* of the animal. This and the reduced responses to repeated application of a drug may be related to tissue receptor desensitization (contrasting denervation hypersensitivity). Thus, on the day of dissection, the tissues may not have been fully relaxed, but after 2 or 3 days in cold saline, the baseline tonus of the walls may have decreased so they become more responsive to drugs. This suggests that the animal can both actively contract and relax vessel walls to control arterial resistance. Since the arteries do not appear to be innervated (M.J.C., K. S. Chan and J.L.W., unpublished), cardioactive drugs must be acting directly on the vessel walls to cause contraction while an unknown relaxing factor, possibly nitric oxide (Mahadevan et al., 2004), circulating in the haemolymph or released by surrounding tissues, could cause vessel dilation. Such local control of arterial radius, plus the participation of cardioarterial valves and DAA-lateral artery valves, will be important in regional haemolymph distribution patterns among the seven arteries leaving the heart (Airriess and McMahon, 1992; Davidson et al., 1998; McGaw and Reiber, 2002; Guadagnoli and Reiber, 2005).

Poiseuille's law states that the drug-induced decreases in vessel radius, measured here, will increase the resistance to flow by the inverse fourth power of that change. Further, since serial resistances are additive, it is obvious that even a very small decrease in radius repeated along the length of an artery and its branches can have a profound effect on flow through that vessel.

The motor that drives circumferential contraction in lobster arteries is probably based on actomyosin interactions. We show above that myosin is clearly present, and actin-containing microfilaments in the cells of these arteries may complete the contractile apparatus (Fig. 2). Three morphological observations on lobster arteries – the presence of prominent bundles of actin-based microfilaments in cells of the tunica intermedia, the association of microfilament bundles with the plasmalemma, and the tendency of microfilament bundles to orient circularly with respect to the vessel lumen – prompted us to investigate the role of microfilaments with cytochalasin D (CD). Pretreatment with CD, a drug that inhibits actin polymerization and disrupts filament organization, reduces or eliminates the slow contractions of both ALA and SA, and it reduces the force generated by OOM. CD inhibits contraction of unstriated smooth muscle (Adler et al., 1983; Saito et al., 1996; Mehta and Gunst, 1999) and cardiac striated muscle (Wu et al., 1998) in vertebrates. Polymerization of globular (G) actin into F-actin may be necessary to force generation in some smooth muscle cells (Adler et al., 1983; Mehta and Gunst, 1999). In the arterial cells and the OOM of the lobster, the filament bundles are obviously pre-existing. However, the density of F-actin depends on the rates of polymerization and depolymerization. CD will shift the balance toward depolymerization and, hence, the density of force-bearing actin filaments may decrease after CD treatment. In addition, CD might also disrupt the normally close spacing of the microfilaments, reducing the probability of cross-bridge formation between myosin and actin molecules.

Quantitative study of transmural arterial pressure and diameter of lobster arteries is still needed, but it is clear from our data that PR and GLU may increase wall stress substantially. To a first approximation, the magnitude of the increased wall stress is sufficient to constrict the arteries *in vivo* (at arterial pressure=1.0 kPa) by ~20% and hence explain the observed increase in the resistance to flow by a factor of two to three (Wilkens, 1997; Wilkens and Taylor, 2003). If these predictions can indeed be corroborated *in vivo*, it will emphasize that PR and GLU play important active roles in the haemodynamics of crustaceans.

## LIST OF ABBREVIATIONS

| | |
|---|---|
| ALA | anterior lateral artery |
| AMA | anterior median artery |
| CD | cytochalasin D |
| DAA | dorsal abdominal artery |
| GLU | glutamic acid |
| HA | hepatic artery |
| OOM | orbicularis ostii muscle |
| PR | proctolin |
| SA | sternal artery |

The authors thank Dr Doug Syme and Dr Manfred Lohka for their helpful insights and suggestions and Ms Lori Anne Archer for assistance with the SDS-PAGE. This work was supported by a personal grant to J.L.W. and research operating funds to M.J.C. from the University of Calgary Research Grants Committee. H.E.D.J.t.K. holds a Medical Scientist award from the Alberta Heritage Foundation for Medical Research.

## REFERENCES

**Adler, K. B., Krill, J., Alberghini, T. V. and Evans, J. N.** (1983). Effect of cytochalasin D on smooth muscle contraction. *Cell Motil.* **3**, 545-551.
**Airriess, C. N. and McMahon, B. R.** (1992). Aminergic modulation of circulatory performance in the crab *Cancer magister*. *Comp. Physiol.* **11**, 123-131.
**Cavey, M. J., Chan, K. S. and Wilkens, J. L.** (2008). Microscopic anatomy of the thin-walled vessels leaving the heart of the lobster *Homarus americanus*: anterior median artery. *Invertebr. Biol.* In press.
**Chan, K. S., Cavey, M. J. and Wilkens, J. L.** (2006). Microscopic anatomy of the thin-walled vessels leaving the heart of the lobster *Homarus americanus*: anterior lateral arteries. *Invertebr. Biol.* **125**, 70-82.
**Cloney, R. A. and Florey, E.** (1968). Ultrastructure of cephalopod chromatophore organs. *Z. Zellforsch. Mikrosk. Anat.* **89**, 250-280.
**Davidson, G. W., Wilkens, J. L. and Lovell, P.** (1998). Neural control of the lateral abdominal arterial valves in the lobster *Homarus americanus*. *Biol. Bull.* **194**, 72-82.
**Factor, J. R.** (1995). The digestive system. In *Biology of the Lobster Homarus americanus* (ed. J. R. Factor), pp. 395-440. San Diego: Academic Press.
**Fujiwara-Tsukamoto, Y., Kuwasawa, K. and Okada, J.** (1992). Anatomy and physiology of neural regulation of haemolymph flow in the lateral arteries of the isopod crustacean, *Bathynomus doederleini*. In *Phylogenetic Models in Functional Coupling of the CNS and Cardiovascular System* (*Comparative Physiology, Vol. 11*) (ed. R. B. Hill and K. Kuwasawa), pp. 70-85. Basel: Karger.
**Guadagnoli, J. A. and Reiber, C. L.** (2005). Changes in cardiac output and hemolymph flow during hypoxic exposure in the gravid grass shrimp, *Palaemonetes pugio*. *J. Comp. Physiol. B* **175**, 313-322.
**Kuramoto, T., Hirose, E. and Tani, M.** (1992). Neuromuscular transmission and hormonal modulation in the cardioarterial valve of the lobster, *Homarus americanus*. In *Phylogenetic Models in Functional Coupling of the CNS and Cardiovascular System* (*Comparative Physiology, Vol. 11*) (ed. R. B. Hill and K. Kuwasawa), pp. 62-69. Basel: Karger.
**Kuramoto, T., Wilkens, J. L. and McMahon, B. R.** (1995). Neural control of cardiac outflow through the sternal valve in the lobster *Homarus americanus*. *Physiol. Zool.* **63**, 443-452.
**Mahadevan, A., Lappé, J., Rhyne, R. T., Cruz-Bermúdez, N. D., Marder, E. and Goy, M. F.** (2004). Nitric oxide inhibits the rate and strength of cardiac contractions in the lobster *Homarus americanus* by acting on the cardiac ganglion. *J. Neurosci.* **24**, 2813-2824.
**Martin, G. G., Hose, J. E. and Corzine, C. J.** (1989). Morphological comparison of major arteries in the ridgeback prawn, *Sicyonia ingentis*. *J. Morphol.* **200**, 175-183.
**McGaw, I. J.** (2005). Does feeding limit cardiovascular modulation in the Dungeness crab *Cancer magister* during hypoxia? *J. Exp. Biol.* **208**, 83-91.
**McGaw, I. J. and Reiber, C. L.** (2000). Integrated physiological responses to feeding in the blue crab *Callinectes sapidus*. *J. Exp. Biol.* **203**, 359-368.
**McGaw, I. J. and Reiber, C. L.** (2002). Cardiovascular system of the blue crab *Callinectes sapidus*. *J. Morphol.* **251**, 1-21.
**McLaughlin, P. A.** (1980). *Comparative Morphology of Recent Crustacea*. San Francisco: W. H. Freeman.
**McMahon, B. R., Wilkens, J. L. and Smith, P. J. S.** (1997). Invertebrate circulatory systems. In *Handbook of Physiology, Section 13, Comparative Physiology* (ed. W. H. Dantzler), pp. 931-1008. New York: Oxford University Press.
**Medler, S. and Mykles, D. L.** (2003). Analysis of myofibrillar proteins and transcripts in adult skeletal muscles of the American lobster *Homarus americanus*: variable expression of myosins, actin and troponins in fast, slow-twitch and slow-tonic fibres. *J. Exp. Biol.* **206**, 3557-3567.
**Mehta, D. and Gunst, S. J.** (1999). Actin polymerization stimulated by contractile activation regulates force development in canine tracheal smooth muscle. *J. Physiol.* **519**, 829-840.
**Meiss, D. E., Lyerla, T. A., Cain, S. and Costello, W. J.** (1981). Electrophoretic protein patterns in fast and slow muscles of the lobster, *Homarus americanus*. *J. Exp. Zool.* **217**, 361-364.
**Mykles, D. L.** (1985). Heterogeneity of myofibrillar proteins in lobster fast and slow muscles: variants of troponin, paramyosin, and myosin light chains comprise four distinct protein assemblages. *J. Exp. Zool.* **234**, 23-32.
**Reynolds, E. S.** (1963). The use of lead citrate at high pH as an electron-opaque stain in electron microscopy. *J. Cell Biol.* **17**, 208-212.
**Saito, S. Y., Hori, M., Ozaki, H. and Karaki, H.** (1996). Cytochalasin D inhibits smooth muscle contraction by directly inhibiting contractile apparatus. *J. Smooth Muscle Res.* **32**, 51-60.
**Shadwick, R. E., Pollock, C. M. and Stricker, S. A.** (1990). Structure and biomechanical properties of crustacean blood vessels. *Physiol. Zool.* **63**, 90-101.
**To, T. H., Brenner, T. L., Cavey, M. J. and Wilkens, J. L.** (2004). Histological organization of the intestine in the crayfish *Procambarus clarkii*. *Acta Zool.* **85**, 119-130.
**Wieland, T.** (1986). *Peptides of Poisonous Amanita Mushrooms*. New York: Springer-Verlag.
**Wilkens, J. L.** (1997). Possible mechanisms of control of vascular resistance in the lobster *Homarus americanus*. *J. Exp. Biol.* **200**, 487-493.
**Wilkens, J. L. and Kuramoto, T.** (1998). Comparison of the roles of neurohormones in the regulation of blood distribution from the hearts of American and Japanese lobsters. *J. Comp. Physiol. B* **168**, 483-490.
**Wilkens, J. L. and Taylor, H. H.** (2003). The control of vascular resistance in the southern rock lobster, *Jasus edwardsii* (Decapoda: Palinuridae). *Comp. Biochem. Physiol.* **135A**, 369-376.
**Wilkens, J. L., Davidson, G. W. and Cavey, M. J.** (1997a). Vascular peripheral resistance and compliance in the lobster *Homarus americanus*. *J. Exp. Biol.* **200**, 477-485.
**Wilkens, J. L., Yazawa, T. and Cavey, M. J.** (1997b). Evolutionary derivation of the American lobster cardiovascular system: an hypothesis based on morphological and physiological evidence. *Invertebr. Biol.* **116**, 30-38.
**Wilkens, J. L., Shinozaki, T., Yazawa, T. and ter Keurs, H. E. D. J.** (2005). Sites and modes of action of proctolin and the FLP $F_2$ on lobster cardiac muscle. *J. Exp. Biol.* **208**, 737-747.
**Wood, R. L. and Luft, J. H.** (1965). The influence of buffer systems on fixation with osmium tetroxide. *J. Ultrastruct. Res.* **12**, 22-45.
**Wu, J., Biermann, M., Rubart, M. and Zipes, D. P.** (1998). Cytochalasin D as excitation-contraction uncoupler for optically mapping action potentials in wedges of ventricular myocardium. *J. Cardiovasc. Electrophysiol.* **9**, 1336-1347.
**Yazawa, T., Wilkens, J. L., ter Keurs, H. E. D. J. and Cavey, M. J.** (1999). Structure and contractile properties of the ostial muscle (musculus orbicularis ostii) in the heart of the American lobster. *J. Comp. Physiol. B* **169**, 529-537.